*Inorg. Chem.* **2007**, *46*, 7232–7234


# Communication in Platinum Ethynylchalcogenophenes

**Emma C. James, Marek Jura, Gabriele Kociok-Köhn, Paul R. Raithby, Emma L. Sharp, and Paul J. Wilson***

*Department of Chemistry, University of Bath, Claverton Down, Bath BA2 7AY, U.K.*

Received April 3, 2007

A series of alkynylchalcogenophene platinum(II) complexes have been synthesized and characterized by multinuclear NMR and UV–visible absorption spectroscopies; the NMR spectra show unprecedented long-range heteronuclear coupling, and clear correlations emerge between spectroscopic data and theoretical analysis of their electronic structures.

Both platinum acetylide complexes[1−3] and purely organic thiophene-based $\pi$-conjugated systems[4] have generated interest in recent years because of their potential applications in molecular electronics. This interest has duly led to examination of platinum acetylide complexes of oligothiophenes.[5] However, no reports on complexes of the higher chalcogenophenes exist despite substitution having been shown to clearly affect molecular properties in solely organic systems.[6,7] To date, only one report describes metal complexes of alkynylselenophenes,[8] where the alkyne C atoms contribute to an $Ir_2M_2C_2$ cluster (M = Mo, W), and a single alkynyltellurophene compound is known.[9] With this in mind, the homologous series of platinum ethynylchalcogenophenes, **1**−**4** (Scheme 1), was synthesized in order to investigate the effect of the chalcogen on their electronic structures and properties.

The usual synthetic route to such species is via a dehydrohalogenation reaction involving a free alkyne and a transition-metal halide in the presence of an amine base, with a copper(I) iodide catalyst under anaerobic conditions.[10] However, such reactions often prove difficult because of thermal or photochemical instability of the free alkyne. Moreover, in the synthesis of **1**−**4**, the free alkyne is highly volatile, and so an in situ deprotection of the silylated alkyne under dehydrohalogenation conditions was developed. The reaction of 2-(trimethylsilyl)ethynylchalcogenophene, sodium methoxide, methanol, and *trans*-$[PtCl_2(P^nBu_3)_2]$ (Scheme 1) affords **1**−**4** in good yield. Notably, omission of methanol hampers the progress of the reaction, implying that the protonated alkyne plays a significant role in the coupling process.

**Scheme 1**[a]

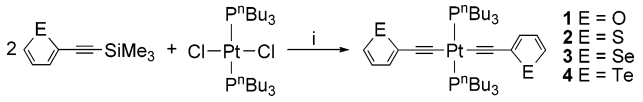


[a] (i) NaOMe, CuI, MeOH, $Et_2NH$, $CH_2Cl_2$, 12−48 h, 72−80%.

The molecular structure of **2**[11] (Figure 1) comprises a pseudo-square-planar *trans*-$PtL_2X_2$ system. The Pt atom lies on a crystallographic center of symmetry, and so the P−Pt−P# and C(13)−Pt−C(13)# angles are linear by symmetry. The orientation of the thiophene ring planes [S(1) C(15) C(16) C(17) C(18)] with respect to the platinum square plane [Pt P P# C(13) C(13)#] is approaching perpendicularity with angles of 74.0°.

Complexes **1**−**4** have been fully characterized by multinuclear NMR spectroscopies. For **3** and **4**, the chalcogen has NMR-active isotopes with $I = {}^1/_2$ and appreciable sensitivities and natural abundances ($^{77}$Se, 7.58%; $^{125}$Te, 6.99%), and indeed the $^1$H NMR spectra for these complexes clearly show proton−chalcogen couplings within the chalocogenophene ring. The $^{31}P\{^1H\}$ NMR spectra of **1**−**4** show only small

* To whom correspondence should be addressed. E-mail: p.j.wilson@bath.ac.uk. Tel: +44 (0)1225 384376.

(1) Long, N. J.; Williams, C. K. *Angew. Chem., Int. Ed.* **2003**, *42* (23), 2586−2617.
(2) Silverman, E. E.; Cardolaccia, T.; Zhao, X. M.; Kim, K. Y.; Haskins-Glusac, K.; Schanze, K. S. *Coord. Chem. Rev.* **2005**, *249* (13−14), 1491−1500.
(3) Vestberg, R.; Westlund, R.; Eriksson, A.; Lopes, C.; Carlsson, M.; Eliasson, B.; Glimsdal, E.; Lindgren, M.; Malmstrom, E. *Macromolecules* **2006**, *39* (6), 2238−2246.
(4) Blanchard, P.; Verlhac, P.; Michaux, L.; Frere, P.; Roncali, J. *Chem.—Eur. J.* **2006**, *12* (4), 1244−1255.
(5) Chawdhury, N.; Kohler, A.; Friend, R. H.; Wong, W. Y.; Lewis, J.; Younus, M.; Raithby, P. R.; Corcoran, T. C.; Al-Mandhary, M. R. A.; Khan, M. S. *J. Chem. Phys.* **1999**, *110* (10), 4963−4970.
(6) Narita, Y.; Hagiri, I.; Takahashi, N.; Takeda, K. *Jpn. J. Appl. Phys.* **2004**, *43* (7A), 4248−4258.
(7) Salzner, U.; Lagowski, J. B.; Pickup, P. G.; Poirier, R. A. *Synth. Met.* **1998**, *96* (3), 177−189.
(8) Notaras, E. G. A.; Lucas, N. T.; Humphrey, M. G.; Willis, A. C.; Rae, A. D. *Organometallics* **2003**, *22* (18), 3659−3670.
(9) Inoue, S.; Jigami, T.; Nozoe, H.; Aso, Y.; Ogura, F.; Otsubo, T. *Heterocycles* **2000**, *52* (1), 159−170.
(10) Khan, M. S.; Al-Mandhary, M. R. A.; Al-Suti, M. K.; Feeder, N.; Nahar, S.; Kohler, A.; Friend, R. H.; Wilson, P. J.; Raithby, P. R. *J. Chem. Soc., Dalton Trans.* **2002**, (12), 2441−2448.

(11) Crystal data for **2**: $C_{36}H_{60}P_2PtS_2$, $M$ = 813.99, pale-yellow block, 0.30 × 0.20 × 0.15 mm, monoclinic, space group $P2_1/c$ (No. 14), $a$ = 10.3320(1) Å, $b$ = 9.2760(1) Å, $c$ = 20.6730(3) Å, α = 99.066-(1)°, $V$ = 1956.54(4) Å$^3$, $Z$ = 2, $D_c$ = 1.382 g cm$^{-3}$, Mo Kα radiation, $\gamma$ = 0.710 73 Å, $T$ = 150(2) K, $\mu$ = 3.796 mm$^{-1}$, $2\theta_{max}$ = 59.98°, 25 529 reflections collected, 5657 unique ($R_{int}$ = 0.0599). Final GOF = 1.054, R1 = 0.0324, wR2 = 0.0841, $R$ indices based on 5657 reflections with $I > 2\sigma(I)$ (refinement on $F^2$), 205 parameters, 0 restraints.



10.1021/ic7006364 CCC: $37.00 
Published on Web 08/10/2007

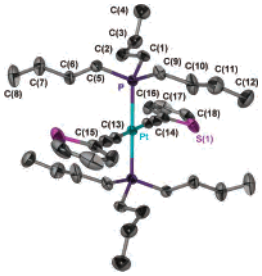


**Figure 1.** Molecular structure of **2**[11] illustrated as a thermal ellipsoid plot (50% probability level). H atoms and atoms corresponding to disorder in the thiophene rings have been omitted for clarity. See the Supporting Information for full structural details.

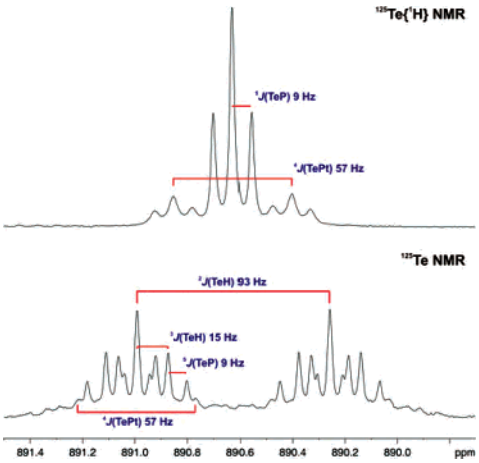


**Figure 2.** $^{125}$Te{$^1$H} and $^{125}$Te NMR spectra of **4** in a $CDCl_3$ solution.

**Table 1.** Selected NMR Spectral Data for **1**−**4** in a $CDCl_3$ Solution

| | $\delta^{31}$P | $^1J_{PtP}$/Hz | $\delta^{195}$Pt | $\delta^{77}$Se/$^{125}$Te | $^4J_{PtE}$/Hz | $^5J_{EP}$/Hz |
|---|---|---|---|---|---|---|
| **1** | 5.42 | 2327 | −4713 | | | |
| **2** | 5.73 | 2339 | −4702 | | | |
| **3** | 5.91 | 2338 | −4688 | 665.7 | 27 | 4.1 |
| **4** | 6.29 | 2343 | −4671 | 890.6 | 57 | 9.0 |

downfield shifts in $\delta^{31}$P from E = O to Te (Table 1). The $^1J(^{195}Pt^{31}P)$ values are typical of a trans platinum bis(phosphine) bis(alkyne) arrangement[12] ($^{195}$Pt: $I = {}^1/_2$, 33.83%) and show little dependence on the identity of the chalcogen, suggesting that the alkyne substituent does not influence the nature of the Pt−P bond significantly (Table 1).

Compounds **3** and **4** have also been characterized by $^{77}$Se/$^{77}$Se{$^1$H} and $^{125}$Te/$^{125}$Te{$^1$H} NMR experiments, respectively. The $^{125}$Te NMR spectrum of **4** (Figure 2) appears complex but clearly shows Te−H coupling, which mirrors that seen in the $^1$H NMR spectrum. $^3J_{TeH}$ involving tellurophene protons in positions 3 and 4 affords a pseudotriplet. The tellurium nuclei also couple to the platinum, $^4J_{PtTe}$ = 57 Hz, and two equivalent phosphorus nuclei, exhibiting a $^5J_{TeP}$ = 9.0 Hz. The $^{125}$Te{$^1$H} NMR spectrum better illustrates this long-range coupling; all coupling constants are consistent throughout the $^1$H, $^{31}$P, $^{125}$Te, and $^{125}$Te{$^1$H} NMR spectra. This is to the best of our knowledge the first observation of any coupling across more than two bonds between $^{77}$Se and $^{31}$P or $^{195}$Pt[13,14] and the first report of $^{195}$Pt−$^{125}$Te and $^{125}$Te−$^{31}$P coupling through more than one bond

(12) Wrackmeyer, B. *Z. Naturforsch, B: Chem. Sci.* **1991**, *46* (1), 35−38.

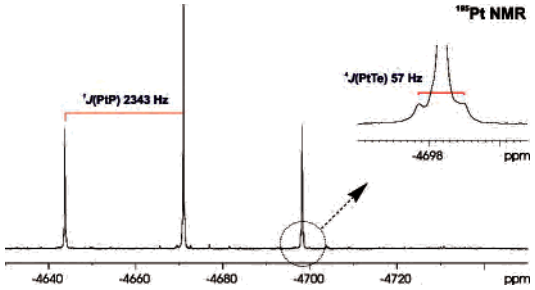


**Figure 3.** $^{195}$Pt{$^1$H} NMR spectra of **4** in a $CDCl_3$ solution.

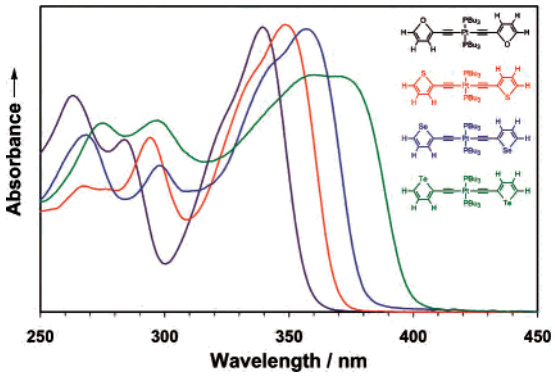


**Figure 4.** Electronic absorption spectra for **1**−**4** in a $CH_2Cl_2$ solution at room temperature.

(for analogous $^{77}$Se/$^{77}$Se{$^1$H} NMR spectra, see Table 1 and the Supporting Information).

The $^{195}$Pt{$^1$H} NMR spectra of **1**−**4** exhibit triplets through coupling to two equivalent phosphorus nuclei (Table 1), as shown for **4** in Figure 3. On closer inspection of the peaks, spin dilute side bands due to tellurium coupling are observed, confirming the $^4J_{PtTe}$ = 57 Hz (see the inset). From E = O to Te, $\delta^{195}$Pt shifts downfield by 42 ppm. The chemical shifts of nuclei are influenced in part by the paramagnetic shielding term $\sigma_{para}$, which dominates when heavy elements are present. $\sigma_{para}$ is inversely proportional to the energy gap between ground and electronic excited states of the molecule (or the gap between occupied and unoccupied molecular orbitals, MOs) due to mixing of the excited-state wavefunction into the ground state. The downfield shift of $\delta^{195}$Pt therefore indicates that the relative magnitude of $\sigma_{para}$ is increasing, and so the relative energy difference between the HOMO and LUMO is decreasing in the order O to Te.

The electronic absorption spectra of **1**−**4** (Figure 4 and Table 2) show that, from E = O to Te, there is a bathochromic (red) shift of $\lambda_{max}$ of the lowest energy optical transition, indicating a decrease in the magnitude of the optical gap, a phenomenon also observed in the parent chalcogenophenes.[15] The high $\epsilon$ values for the transitions imply significant degrees of charge-transfer character, and evidence for strong vibronic coupling is provided by the observation of shoulders to higher energy.

To further investigate the electronic structure of **1**−**4**, theoretical calculations have been carried out using density

(13) Tattershall, B. W.; Sandham, E. L. *J. Chem. Soc., Dalton Trans.* **2001**, (12), 1834−1840.
(14) Harris, R. K.; Mann, B. E. *NMR and the Periodic Table*; Academic Press: London, 1978.
(15) Fringuelli, F.; Taticchi, A. *J. Chem. Soc., Perkin Trans. 1* **1972**, (2), 199−203.

**Table 2.** Observed Electronic Absorption Data for **1**−**4** in a $CH_2Cl_2$ Solution and Calculated Data for the Equivalent Model Compounds **1′**−**4′**

| | observed | | | | calculated | | |
|---|---|---|---|---|---|---|---|
| | $\lambda_{max}$/nm | energy/eV | $\epsilon$/$M^{-1}$ $cm^{-1}$ | | excitation wavelength/nm | excitation energy/eV | oscillator strength (*f*) |
| **1** | 340 | 3.65 | 32 600 | **1′** | 365 | 3.40 | 0.697 |
| **2** | 349 | 3.55 | 32 900 | **2′** | 376 | 3.30 | 0.774 |
| **3** | 357 | 3.47 | 32 400 | **3′** | 385 | 3.22 | 0.783 |
| **4** | 360, 371 | 3.44, 3.34 | 27 200, 27 000 | **4′** | 397 | 3.13 | 0.731 |

functional theory (DFT) using *Gaussian03*[16] on the model compounds *trans*-$PtL_2(PMe_3)_2$, **1′**−**4′**, under $C_i$ symmetry (see the Supporting Information). It is worth noting that a $PH_3$ model of **2** has previously been reported.[17] The potential energy surfaces of **1′**−**4′** exhibit shallow energy minima for geometries in which the chalcogenophene and platinum square planes are practically coplanar.

The frontier MOs for **1′** (Figure 5) show that the HOMO is mainly comprised of the ethynylchalcogenophene $\pi$ orbitals in an out-of-phase combination with the Pt $5d_{xz}$ orbital; contribution from the E $np_z$ orbitals to the HOMO is low. Conversely, the LUMO is largely based on the empty Pt $6p_z$ orbital in phase with both the ethynylchalcogenophene and P $\pi^*$ orbitals. The frontier MOs calculated for **2′**−**4′** are directly analogous to those illustrated for **1′**. However, a decrease in the energy of the LUMO in the order O to Te is observed as a result of decreasing antibonding interactions between the C $2p_z$ and E $np_z$ orbitals, whereas the energy level of the HOMO is less affected. Consequently, there is an overall decrease in the HOMO−LUMO energy gap from E = O to Te. This decrease correlates with the optical gap trend seen in the UV−visible spectra of **1**−**4** and also provides evidence for the relative chemical shift trends observed in the $^{195}$Pt and $^{31}$P NMR spectra of the complexes.

Time-dependent DFT (TDDFT)[18] calculations yielded vertical transition energies of high oscillator strength corresponding predominately to the HOMO to LUMO gap transition for each of the four models (Table 2). The correlation between the calculated excitation wavelength and the experimentally observed *onset of absorption*, i.e., that which does not involve a change of the vibrational or rotational state of the molecule, appears excellent and clearly confirms the delocalization of the frontier MOs across the whole of the molecular $\pi$ system. TDDFT calculations also substantiate the charge-transfer character of the experimentally observed lowest-energy transition because the HOMO is primarily a ligand-based orbital and the LUMO is dominated by the Pt $6p_z$ orbital.

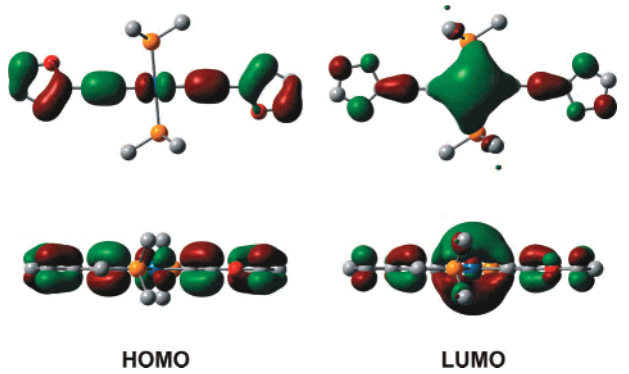


**Figure 5.** MO plots for the frontier MOs of **1′**. (H atoms have been omitted for clarity.)

In addition, the DFT calculations imply free rotation about the alkyne bonds in the molecules, with no particular strong preferences observed for alignment of the ethynylchalcogenophene ligand with or perpendicular to the platinum square plane.[19] Thus, returning to the unusual $^5J_{EP}$ couplings, there is a clear indication that the values observed are averages over all rotamers observed in solution. Indeed, one can consider the P−Pt−$C_{ipso}$−E long-range dihedral angle, $\phi$, to be analogous to the Karplus vicinal dihedral angle in purely organic systems. However, when the dihedral angle is $\phi$, there will always be an equivalent relationship in existence with the other Pt−P vector of 180−$\phi$, and given that the two phosphorus centers are chemically equivalent, an *average* coupling constant will be observed for any possible rotamer. The $^5J_{EP}$ and $^4J_{PtE}$ couplings observed in these systems are very large given both the internuclear distances involved and the ∼90° angle at platinum that is encountered in the five-bond coupling. Given that coupling between nuclei is dominated by their interaction with electrons in the s orbitals that contribute to the bonding MOs, the high s character in the hybridization of the carbon and chalcogen centers must play a significant role.

In conclusion, the first homologous series of ethynylchalcogenophenes and their platinum complexes have been prepared via a developed in situ deprotection−dehydrohalogenation reaction. Unprecedented long-range heteronuclear coupling has been observed in the NMR spectra of the complexes, evidencing strong electronic and nuclear communication. An elegant synergy is also demonstrated between experiment and theory in the investigation of molecular electronic structures.

**Acknowledgment.** The Royal Society (URF to P.J.W.) and the EPSRC (E.L.S.) are acknowledged for financial support. Prof. M. H. Chisholm and the Ohio Supercomputer Center are thanked for computational resources (PAS0259). Dr J. P. Lowe is thanked for assistance with NMR experiments and Johnson Matthey plc for the loan of platinum salts.

**Supporting Information Available:** Synthetic, calculational, and spectroscopic details including $^{77}$Se NMR spectra of **3** and full details of the molecular structure of **2**. This material is available free of charge via the Internet at http://pubs.acs.org.

IC7006364

(16) Frisch, M. J.; Trucks, G. W.; Schlegel, H. B.; et al. *Gaussian03*, revision C.02; Gaussian, Inc.: Wallingford, CT, 2004.
(17) Norman, P.; Cronstrand, P.; Ericsson, J. *Chem. Phys.* **2002**, *285* (2−3), 207−220.
(18) Stratmann, R. E.; Scuseria, G. E.; Frisch, M. J. *J. Chem. Phys.* **1998**, *109* (19), 8218−8224.
(19) Glusac, K.; Kose, M. E.; Jiang, H.; Schanze, K. S. *J. Phys. Chem. B* **2007**, *111* (5), 929−940.